Bull. Mater. Sci., Vol. 40, No. 6, October 2017, pp. 1087–1096
DOI 10.1007/s12034-017-1475-0

Structural stability and magnetic properties of Cu_mCo_nNO ($m + n = 2$–7) clusters

PEI-YING HUO, XIU-RONG ZHANG*, JUN ZHU and ZHI-CHENG YU
School of Mathematics and Physics, Jiangsu University of Science and Technology, Zhenjiang 212003, China
*Author for correspondence (zh4403701@126.com)

MS received 15 December 2016; accepted 27 February 2017; published online 27 September 2017

Abstract. A theoretical study of NO adsorption on Cu_mCo_n ($2 \leq m + n \leq 7$) clusters was carried out using a density functional method. Generally, NO is absorbed at the top site via the N atom, except in Cu_3NO and Cu_5NO clusters, where NO is located at the bridge site. Co_2NO, Co_3NO, Cu_2Co_2NO, Co_5NO, Cu_2Co_4NO and Cu_6CoNO clusters have larger adsorption energies, indicating that NO of these clusters are more easily adsorbed. After adsorption, N–O bond is weakened and the activity is enhanced as a result of vibration frequency of N–O bond getting lower than that of a single NO molecule. Cu_2CoNO, Cu_3CoNO, Cu_2Co_2NO, Cu_3Co_3NO and $CuCo_5NO$ clusters are more stable than their neighbours, while $CuCoNO$, Co_3NO, Cu_3CoNO, Cu_2Co_3NO, Cu_3Co_3NO and Cu_6CoNO clusters display stronger chemical stability. Magnetic and electronic properties are also discussed. The magnetic moment is affected by charge transfer and the spd hybridization.

Keywords. Cu_mCo_nNO ($m + n = 2$–7) clusters; structural stability; magnetic properties; adsorption properties.

1. Introduction

Nitrogen oxides (NO_x) are the major air pollutants, which are harmful to human health. Hence, effective elimination of nitrogen oxides from emission has been an important topic of study for the researchers. A wide variety of metals adsorbing nitrogen oxides has been studied so far [1–6]. Endou *et al* [7] investigated the adsorption and activation properties of precious metals such as Ir, Pt and Au towards NO by means of density functional calculations. They found that the metals arranged in decreasing order of stability after NO adsorption is Ir > Pt > Au, and generally the adsorption state in the on-top model was more stable than those on 3-fold sites. Matulis *et al* [8] studied NO adsorption on neutral, anionic and cationic Ag_8 clusters by considering three cluster types: D_{2d}, T_d and C_1 structures. It has been shown that in the case of NO interaction with D_{2d} structure the corresponding adsorption energies increase in the following order: E_{ads} (cation) < E_{ads} (neutral) < E_{ads} (anion), whereas for the C_1 structure the order is E_{ads} (anion) < E_{ads} (cation) < E_{ads} (neutral). Theoretical study of nitrogen monoxide adsorption on small Si_x ($x = 3$–5) clusters has been carried out by Nahali and Gobal [9] using the method of advanced hybrid meta-density functional method of Truhlar (MPW1B95), which showed that NO prefers adsorption through the nitrogen side. Reconstruction in Si_5 cluster and change of the charge distribution in Si_3 cause large adsorption energies. Valadbeigi *et al* [10] studied properties of CO, N_2, H_2O, O_2, H_2 and NO adsorbing on B_{36} nanocluster. The study indicated that the adsorption properties of CO, O_2 and NO are better than those of other gases; moreover, CO and NO were adsorbed, respectively, via C atom and N atom. When NO and O_2 are adsorbed synchronously via both atoms, they dissociate. Boron atoms at the edge of the B_{36} cluster showed more reactivity than those of the inner atoms.

In recent years, researchers have focused their attention on bimetallic clusters, whose properties are possibly different from those of pure clusters due to their complex structures and factors [11–16]. Qin *et al* [17] investigated the geometry and magnetic properties of Co_mAl_n ($m + n \leq 6$) bimetallic clusters using density functional theory (DFT)-GGA of the $DMOL^3$ package. The most stable structures were similar to pure cobalt clusters. The average magnetic moment decreases linearly with the increase of cobalt atoms, as a result of the weakening of Co atomic spin polarization after the doping of non-magnetic Al atoms. Lu *et al* [18] carried out a study of Cu, Pt, Cu, Cu–Cu and Co–Pt clusters containing 13 atoms. Geometrical analysis of bimetallic Co–Cu and Co–Pt clusters indicated that the structures of bimetallic clusters were slightly distorted configuration of Co_{13}. The total magnetic moment of Co–Pt clusters monotonously decreases with increasing concentration of Pt atoms. Lv *et al* [19] investigated the geometries and stabilities as well as electronic and magnetic properties of Co_nRh ($n = 1$–8) clusters systematically within the framework of the gradient approximation DFT. The results indicated that the most stable structures were similar to those of corresponding Co_{n+1} clusters. The magnetism of the ground state of all alloy clusters displayed ferromagnetic coupling except for Co_3Rh.

However, NO adsorption on Cu–Co bimetallic clusters has received little attention. In this work, the geometrical

configuration, stability, adsorption properties and magnetic properties of the NO molecules adsorbed on Cu_mCo_n ($2 \leq m+n \leq 7$) clusters are studied, which may provide a research foundation for application of mechanism of NO adsorption on Cu–Co alloy clusters.

2. Computational method

All calculations were performed using DFT in the DMOL^3 package of the Materials Studio by Accelrys Inc. The exchange correlation interaction was treated within the GGA using the PW91 function (GGA-PW91). The double numerical basis set augmented with d-polarization functions (DND) was utilized. In the process of geometric optimization, convergence thresholds were set to be 2.0×10^{-5} Hartree (Ha) for the energy, 0.0004 Hartree/Å for the forces and 0.005 Å for the displacement. All of the possible spin multiplicities of each initial configuration were considered to ensure that the obtained structures are the lowest in energy. In order to speed up the self-consistent field (SCF) convergence, the direct inversion in an iterative subspace (DIIS) approach was used. The convergence criterion of SCF was set to be 10^{-5} Ha. We considered the smearing in calculations, and the smearing of molecular orbital occupation was set to be 0.005 Ha. All calculations were spin-unrestricted, which implies that the optimized geometry, electronic structure and magnetic properties were calculated taking full account of spin multiplicity.

3. Results and discussion

3.1 *Geometrical structures*

All the structures were obtained by the methods discussed in Section 2.The lowest-energy configurations with positive frequencies were regarded as the ground-state structures, listed in figure 1. The spin multiplicities and symmetry are also labelled below the structures of figure 1.

For Cu_mCo_nNO ($m+n=2$) clusters, the ground-state structures were obtained based on the linear structures with the NO molecules located at the apex via N side. Bond lengths of Cu–Cu, Cu–Co and Co–Co are 2.25, 2.26 and 2.27 Å, respectively, from which it can be clearly seen that as the number of Co atom increases, the bond length of alloy clusters increases. The clusters are all C_s symmetric with multiplicity 2.

NO are all adsorbed at the top site for Cu_mCo_nNO ($m+n=3$) clusters except in Cu_3NO. In the Cu_3NO cluster, NO is adsorbed at the bridge site on the basis of an isosceles triangle whose waist length is 2.39 Å and base length is 2.57 Å. The ground-state structures of Cu_2CoNO, $CuCo_2NO$ and Co_3NO clusters are C_s symmetric, and their alloy clusters have fold-line structures. Especially in the Co_3NO cluster, the angle of Co–Co–Co changes considerably from 80.00 to 56.88° after adsorption.

In the case of Cu_mCo_nNO ($m+n=4$) clusters, the ground-state structures are all non-planar quadrilaterals with NO adsorption at the top site through the N atom. In particular, the structure of Cu_4NO cluster is based on a regular tetrahedron whose bond length is 2.43 Å. After adsorption, one Cu–Cu bond is significantly elongated, leading to a significant change in the configuration. Hence, it indicates that for the clusters containing 4 Cu atoms, the ground state tends to be a planar structure. For Cu_3CoNO, Cu_2Co_2NO, $CuCo_3NO$ and Co_4NO clusters, NO is adsorbed on the Co atoms located at the short diagonal. With the increasing Co atoms, it can be seen that Cu atom in the original configuration is replaced by Co atom. Its symmetry is C_{2v}, C_1, C_{2v} and C_{2v}, correspondingly.

Before adsorption, the ground state of Cu_5 cluster has a planar structure formed by three different triangles with C_s symmetry. When NO is adsorbed at the bridge site of Cu_5 cluster, the length of Cu–Cu bond is changed. The middle triangle becomes an isosceles triangle with 2.45 Å waist length and 2.51 Å base length, while the other two triangles are symmetrically distributed on both sides of the isosceles triangle with the same shape. The Cu–N bond is 1.91 Å in length and the multiplicity is 3. The lowest-energy structures of Cu_4CoNO and Cu_3Co_2NO were obtained on the basis of a slightly twisted quadrangular pyramid. NO adsorption leads to a distortion of the trigonal bipyramidal structure, in which NO is adsorbed on Co atom through the N side. The multiplicity and symmetry of Cu_4CoNO and Cu_3Co_2NO are 1, C_{2v} and 3, C_s, respectively. The ground-state configurations of $CuCo_5$ and Co_6 clusters are both trigonal bipyramidal, and the adsorption of NO does not change its configuration much.

For Cu_mCo_nNO ($m+n=6$) clusters, the ground-state structures of Cu_6NO, Cu_5CoNO, Cu_4Co_2NO and Cu_2Co_4NO clusters are all based on a single-cap trigonal bipyramidal configuration with NO adsorption. The multiplicity is 2, 2, 4 and 8, correspondingly. Cu_3Co_3 has a tetragonal bipyramid structure. A Cu–Cu bond located in the bottom is significantly elongated after NO adsorption, resulting in a configuration change of a single-capped trigonal bipyramidal structure. For $CuCo_5NO$ and Co_6NO clusters, NO are on Co atoms of tetragonal bipyramid with top-site adsorption.

For Cu_mCo_nNO ($m+n=7$), the obtained configurations of Cu_7NO, $CuCo_6NO$ and Co_7NO are all on the basis of tetragonal bipyramid structures, in which NO molecules are adsorbed on top sites. The ground state structures of $CuCo_6$ and Co_7 were obtained on the basis of Cu7 cluster with Cu atoms are replaced by Co atoms. The configurations have C_s, C_1 and C_1 symmetry with the multiplicities of 1, 9 and 7, correspondingly. For Cu_6CoNO, Cu_5Co_2NO and Cu_3Co_4NO clusters, the lowest-energy structures are obtained based on the pentagonal bipyramid structure, which can be seen as Co atoms replacing Cu atoms in the D_{5h} symmetric pentagonal bipyramid structure. It can be seen from figure 1 that the Co atoms are more inclined to replace the Cu atoms at the centre of the pentagonal bipyramid structure. However, the Cu_4Co_3NO and Cu_2Co_5NO structures are built on double-capped trigonal

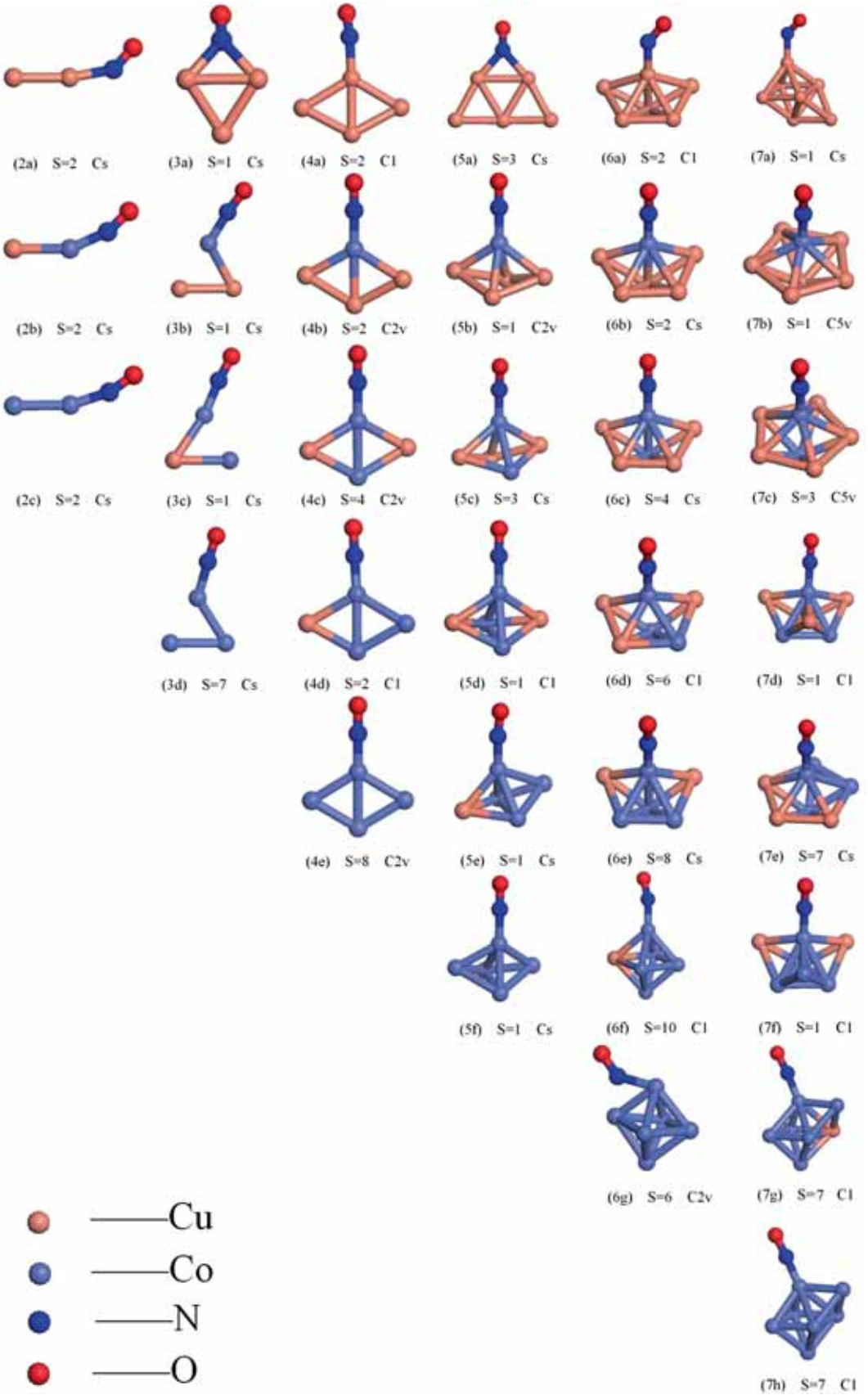

Figure 1. The ground-state structures of Cu_mCo_nNO ($2 \leq m + n \leq 7$) clusters.

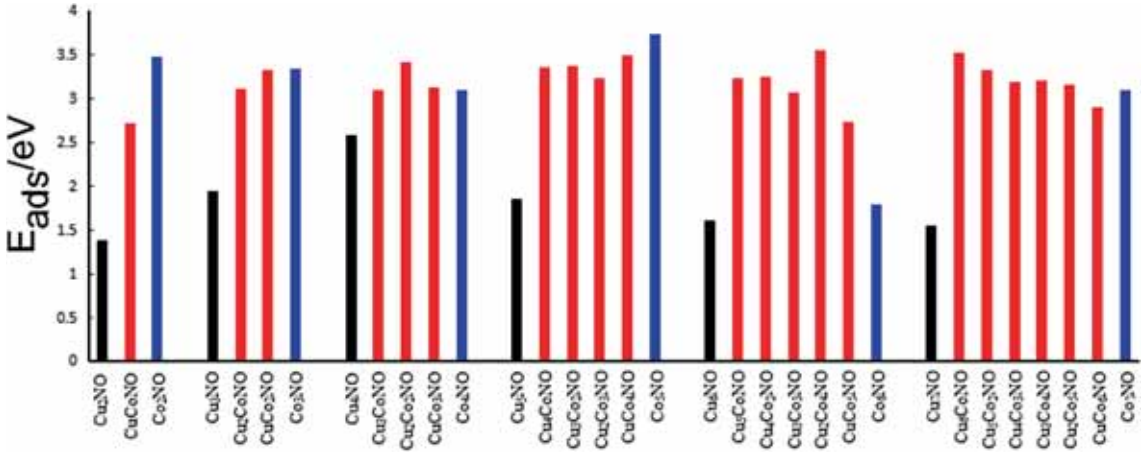

Figure 2. The adsorption energies of Cu_mCo_nNO ($2 \leq m + n \leq 7$) clusters at ground state.

bipyramidal structure. The symmetry and multiplicity of the two clusters are the same, which are C_1 and 1, respectively.

3.2 *Adsorption strength*

In order to study adsorption strength of clusters, the adsorption energies are analysed, which can indicate the interaction of clusters and NO molecules. Larger the adsorption energy, easier the NO can adsorption on the surface of clusters, indicating that combination between NO molecule and alloy clusters is stronger. Adsorption energies can be calculated as follows:

$$E_{\text{ads}} = E(\text{NO}) + E(\text{Cu}_m\text{Co}_n) - E(\text{Cu}_m\text{Co}_n\text{NO}).$$

The adsorption energy curves of Cu_mCo_nNO ($2 \leq m+n \leq 7$) clusters are shown in figure 2, where black, red and blue bars correspond to Cu, Cu–Co and Co clusters, respectively. As figure 2 indicates, the adsorption energies of pure Cu clusters are generally lower, which means that the interaction of Cu clusters and NO molecule is relatively smaller. Co_2NO, Co_3NO, Cu_2Co_2NO, Co_5NO, Cu_2Co_4NO and Cu_6CoNO clusters have the peak adsorption energy, indicating that the combination of NO molecules is better here than in their neighbours. The adsorption energy of Co_5NO is the largest, which implies that NO molecule is more likely to be adsorbed on the surface of Co_5 cluster, and the interaction of Co_5 cluster and NO is the strongest.

The NO charge, the Cu–Co–N bond length and N–O vibration frequency are listed in table 1 for the ground-state structures of Cu_mCo_nNO ($2 \leq m + n \leq 7$) clusters. Among the NO studied, NO of Cu_mNO ($m = 1$–7) and Co_6NO clusters are all negatively charged. It indicates charge transfer from alloy clusters to NO molecules, resulting in longer N–O bond. Hence, N–O bonds of Cu_mNO ($m = 1$–7) and Co_6NO clusters are weakened and the activities of NO molecules are strengthened, which agrees well with N–O bond length listed in table 1. As table 1 shows, N–O bond lengths of Cu_mNO clusters are all larger than those of cobalt-doped clusters, indicating that the N–O bonds of Cu_mNO clusters are weaker and NO activities are higher. The length of N–O is between 1.181 and 1.192 Å for the clusters where NO is adsorbed at the top site. When NO is adsorbed at the bridge site, the N–O bond is elongated to more than 1.220 Å. When compared with studies of NO adsorption on Pd_n, Ag_n and Cu_n clusters [20,21], it can be found that N–O bonds of Cu_mCo_nNO clusters are longer; hence, it implies that the activities of NO molecules here are larger. The degree of charge transfer can reflect the strength of the bond to some extent. It can be easily found that the amount of charge transfer in Cu_6CoNO, Cu_5CoNO, Cu_5Co_2NO and Cu_4Co_3NO clusters is, respectively, 0.127, 0.103, 0.105 and 0.104e, which are significantly greater than others, illustrating that Cu_6Co-NO, Cu_5Co-NO, Cu_5Co_2−NO and Cu_4Co_3–NO bonds are stronger.

In cluster research, vibration frequency is often used to study interaction strength of bonding atoms. The higher the vibration frequency, the stronger the interaction. As shown in table 1, vibration frequencies of N–O bonds are all lower than the single NO molecule vibration frequency of 1890.500 cm^{-1}, indicating that N–O bond is weakened and the activity is enhanced after adsorption.

3.3 *Stability*

Second-order energy difference ($\Delta_2 E$) is analysed to describe cluster stability. The larger this value, the more stable the corresponding cluster. The calculation formula is as follows:

$$\begin{aligned}\Delta_2 E_n &= E(\text{Cu}_m\text{Co}_{n+1}\text{NO}) + E(\text{Cu}_m\text{Co}_{n-1}\text{NO}) \\ &\quad -2E(\text{Cu}_m\text{Co}_n\text{NO}), \\ \Delta_2 E_m &= E(\text{Cu}_{m+1}\text{Co}_n\text{NO}) + E(\text{Cu}_{m-1}\text{Co}_n\text{NO}) \\ &\quad -2E(\text{Cu}_m\text{Co}_n\text{NO}).\end{aligned}$$

Table 1. The charge of NO(Q_{NO}), the length of Cu–Co–N and N–O bond ($L_{Cu-Co-N}$ and L_{N-O} respectively), N–O vibration frequency.

$m+n$	Cluster	Q_{NO} (e)	$L_{Cu-Co-N}$ (Å)	L_{N-O} (Å)	N–O vibration frequency (cm^{-1})
2	Cu_2NO	−0.001	1.809	1.187	1715.940
	CuCoNO	0.084	1.649	1.181	1804.110
	Co_2NO	0.059	1.648	1.183	1798.070
3	Cu_3NO	−0.163	1.920	1.215	1503.350
	Cu_2CoNO	0.072	1.628	1.185	1788.040
	$CuCo_2NO$	0.063	1.634	1.186	1784.040
	Co_3NO	0.037	1.647	1.187	1787.190
4	Cu_4NO	−0.037	1.787	1.190	1689.610
	Cu_3CoNO	0.099	1.631	1.181	1813.030
	Cu_2Co_2NO	0.088	1.630	1.183	1802.120
	$CuCo_3NO$	0.077	1.630	1.185	1792.280
	Co_4NO	0.079	1.629	1.186	1785.890
5	Cu_5NO	−0.222	1.914	1.237	1445.000
	Cu_4CoNO	0.073	1.628	1.184	1794.460
	Cu_3Co_2NO	0.060	1.626	1.185	1790.290
	Cu_2Co_3NO	0.072	1.621	1.187	1776.380
	$CuCo_4NO$	0.038	1.629	1.188	1773.770
	Co_5NO	0.055	1.631	1.187	1778.740
6	Cu_6NO	−0.056	1.804	1.192	1669.850
	Cu_5CoNO	0.103	1.624	1.182	1797.250
	Cu_4Co_2NO	0.090	1.625	1.183	1791.490
	Cu_3Co_3NO	0.089	1.621	1.185	1782.290
	Cu_2Co_4NO	0.078	1.620	1.186	1782.380
	$CuCo_5NO$	0.060	1.628	1.188	1763.790
	Co_6NO	−0.040	1.805	1.222	1521.380
7	Cu_7NO	−0.023	1.789	1.187	1678.440
	Cu_6CoNO	0.127	1.604	1.184	1803.460
	Cu_5Co_2NO	0.105	1.613	1.184	1794.620
	Cu_4Co_3NO	0.104	1.619	1.186	1782.230
	Cu_3Co_4NO	0.093	1.620	1.186	1779.520
	Cu_2Co_5NO	0.093	1.622	1.187	1770.960
	$CuCo_6NO$	0.074	1.627	1.189	1623.120
	Co_7NO	0.073	1.629	1.188	1768.510

For a fuller discussion of the stability, the second-order energy differences are analysed by considering Cu atom and Co atom as variables in figures 3 and 4, respectively. In figure 3 the curves of Cu_mCo_nNO ($n = 1$–7) are plotted, which show significant odd–even oscillations. For pure Co clusters, maxima are found at $n = 6$; hence, Co_6NO is more stable. Clusters containing an odd number of Cu atoms or odd number of Co atoms correspond to peaks. The trend is opposite in clusters containing an even number of Cu atoms. In figure 4, Cu_5NO is more stable for pure Cu clusters. For clusters doped with odd number of Co atoms, peaks are located when m is odd. The trend is opposite for clusters doped with even number of Co atoms. On the whole, combining figures 3 and 4, the Δ_2E values of Cu_2CoNO, Cu_3CoNO, Cu_2Co_2NO, Cu_3Co_3NO and $CuCo_5NO$ clusters are much larger than those of other clusters, indicating that these five clusters are much more stable.

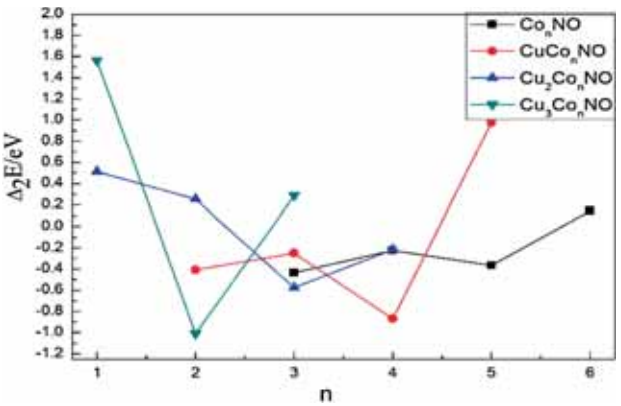

Figure 3. Second-order energy differences of the ground-state structures of Cu_mCo_nNO clusters as a function of the number of Co atoms.

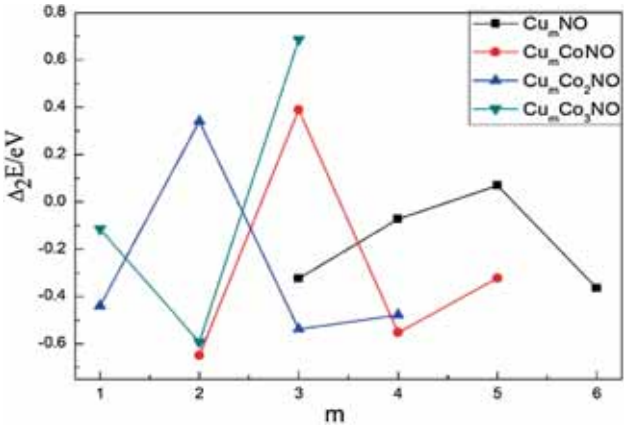

Figure 4. Second-order energy differences of the ground-state structures of Cu_mCo_nNO clusters as a function of the number of Cu atoms.

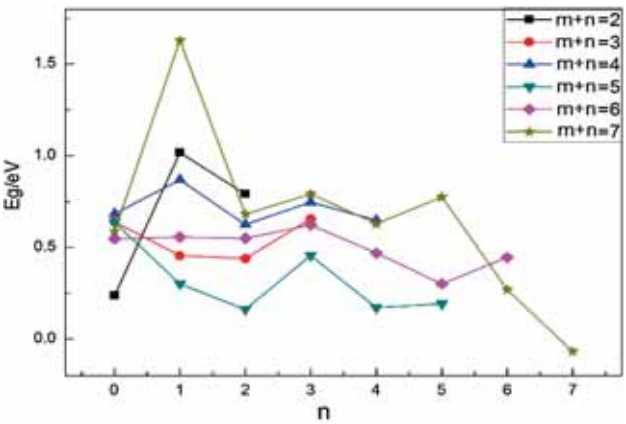

Figure 5. The energy gap of Cu_mCo_nNO ($2 \leq m+n \leq 7$) clusters at ground state.

The energy gap (E_g) can reflect the chemical stability and activity of clusters, which can be expressed as

$$E_g = E_{LUMO} - E_{HOMO}.$$

Higher the gap value, worse the chemical activity of cluster and stronger the chemical stability. The curves of HOMO–LUMO gap of Cu_mCo_nNO ($2 \leq m+n \leq 7$) clusters are plotted in figure 5, in which odd–even oscillation can be clearly found with the increase of Co atoms under the same size. The peaks correspond to the clusters where the number of Co atoms is odd, indicating stronger chemical stability and worse chemical activity. In different sizes, CuCoNO, Co_3NO, Cu_3CoNO, Cu_2Co_3NO, Cu_3Co_3NO and Cu_6CoNO clusters display higher energy gaps, which means that the chemical stability of these clusters is stronger compared with neighbouring clusters.

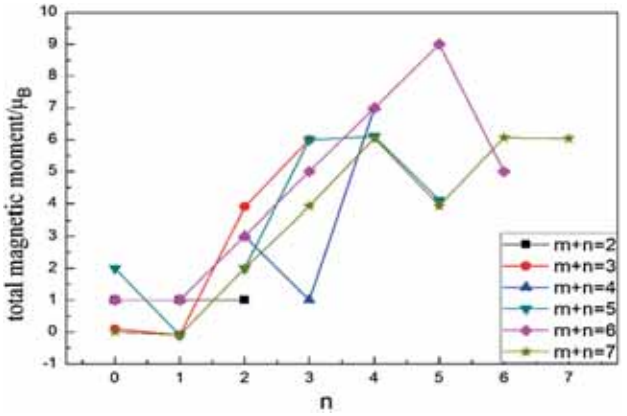

Figure 6. Total magnetic moment of Cu_mCo_nNO ($2 \leq m+n \leq 7$) clusters at ground state.

3.4 *The magnetic and electronic properties*

In figure 6, total magnetic moment of ground-state configurations is plotted as a function of Co concentration for different cluster sizes. It shows that generally the magnetic moments increase as the number of Co atoms doped in pure Cu clusters increases. When only one Co atom is doped, the magnetic moments of the clusters are unchanged. For Cu_mCo_nNO ($m+n=2$) clusters, total magnetic moments of the ground-state configurations are all 1, indicating that doped cobalt atom has no effect for very small size clusters.

In order to explore the magnetic properties, Cu_mCo_nNO ($m+n=6$) clusters are mainly discussed as representatives. Table 2 lists the Mulliken populations of charge, local and total magnetic moment of Cu_mCo_nNO ($m+n=6$) clusters in ground state, and its atomic numbers are labelled in figure 8. It is obvious that the total magnetic moment is mainly from Co atoms. The d orbits show considerable charges, and the magnetic moment mainly arises from localization of the d-electrons. The contribution of p orbits is quite small, which can be ignored. The 4s orbits of Co atoms lose charges, and the 4p,3d orbits get charges. This implies that in the Co atoms, charges are transferred from 4s orbits to 4p,3d orbits, leading to the spd-orbital hybridization. In analysing the atom charges, it can be found that a part of charges is transferred from Co atoms to Cu atoms. Moreover, charge transfer between Co atoms can also be found. To summarize, charge transfer not only occurs between different orbits but also occurs between different atoms, indicating that spd hybridization has taken place in the system. This hybridization changes the original electron pairing and affects the magnetic moment.

For a further magnetism analysis, the partial density of states (PDOS) of Cu_mCo_nNO ($m+n=6$) clusters is also analysed in figure 7. We explored the PDOS from the contribution of different orbitals components. The majority (spin-up) density is plotted as positive and the minority (spin-down) density is plotted as negative. The cluster Fermi level

Table 2. The Mulliken populations of charge and local and total magnetic moment of Cu_mCo_nNO ($m + n = 6$) clusters at ground state.

				Local magnetic moment (μ_B)			Mulliken charge		
Cluster	Atom label	Q	μ_{atom}	3d	4s/3s	4p/3p	3d	4s/3s	4p/3p
Cu_5CoNO	Cu(1)	0.057	0.007	0.006	–0.007/0.000	0.008/0.000	9.770	0.820/1.999	0.357/5.997
	Co(2)	–0.075	1.054	1.020	0.002/0.000	0.034/–0.001	7.731	0.784/2.000	0.558/6.002
	Cu(3),(4)	–0.036	0.016	0.009	0.017/0.000	–0.010/0.000	9.794	0.986/2.000	0.259/5.998
	Cu(5),(6)	–0.056	0.039	0.038	–0.003/0.000	0.005/0.000	9.807	1.065/2.000	0.187/5.998
Cu_4Co_2NO	Co(1)	–0.092	0.973	0.970	–0.012/0.000	0.016/–0.001	7.744	0.798/2.000	0.547/6.002
	Co(2)	0.101	2.050	1.917	0.081/–0.001	0.055/–0.002	7.787	0.319/2.001	0.785/6.006
	Cu(3),(4)	–0.041	0.044	0.026	0.032/0.000	–0.014/0.000	9.788	0.264/2.000	0.992/5.997
	Cu(5),(6)	–0.059	0.054	0.052	–0.002/0.000	0.004/0.000	9.797	1.071/2.000	0.194/5.998
Cu_3Co_3NO	Cu(1)	–0.033	0.094	0.055	0.044/0.000	–0.005/0.000	9.769	1.000/2.000	0.267/5.997
	Co(2)	0.070	2.083	1.964	0.074/–0.001	0.048/–0.003	7.755	0.829/2.001	0.339/6.006
	Cu(3)	–0.052	0.079	0.051	0.038/0.000	–0.010/0.000	9.793	1.054/2.000	0.208/5.998
	Co(4)	0.050	2.388	2.206	0.136/–0.001	0.049/–0.002	7.634	1.030/2.001	0.282/6.004
	Cu(5)	–0.066	0.039	0.064	–0.031/0.000	0.005/0.000	9.783	1.094/2.000	0.191/5.998
	Co(6)	–0.158	0.533	0.557	–0.012/0.000	–0.011/–0.001	7.860	0.785/2.000	0.511/6.001
Cu_2Co_4NO	Co(1)	0.080	2.074	1.982	0.059/–0.001	0.037/–0.003	7.748	0.819/2.001	0.345/6.006
	Co(2)	–0.138	0.656	0.708	–0.021/0.000	–0.029/–0.001	7.808	0.801/2.000	0.528/6.002
	Co(3),(4)	0.001	2.182	2.056	0.100/–0.001	0.029/–0.003	7.727	0.998/2.001	0.268/6.005
	Cu(5),(6)	–0.061	0.111	0.079	0.025/0.000	0.007/0.000	9.778	1.091/2.000	0.195/5.998
$CuCo_5NO$	Co(1)	0.049	2.082	1.986	0.057/–0.001	0.042/–0.003	7.769	0.856/2.001	0.320/6.006
	Co(2)	–0.008	2.137	1.980	0.133/–0.001	0.028/–0.003	7.731	0.996/2.001	0.275/6.005
	Co(3)	–0.160	0.693	0.740	–0.017/0.000	–0.028/–0.002	7.803	0.858/2.000	0.498/6.001
	Co(4)	–0.010	2.124	1.971	0.130/–0.001	0.027/–0.003	7.736	0.994/2.001	0.274/6.005
	Cu(5)	–0.037	0.123	0.091	0.051/0.000	–0.020/0.000	9.716	1.049/2.000	0.275/5.997
	Co(6)	0.004	2.167	2.001	0.145/–0.001	0.025/–0.003	7.729	0.980/2.001	0.283/6.005
Co_6NO	Co(1)	–0.001	–0.941	–0.890	0.002/0.000	–0.054/0.001	7.818	0.783/2.001	0.392/6.007
	Co(2)	0.001	2.073	1.922	0.105/–0.001	0.049/–0.003	7.720	0.982/2.001	0.292/6.005
	Co(3)	–0.038	–1.682	–1.667	0.022/0.000	–0.039/0.002	7.747	1.030/2.001	0.255/6.006
	Co(4)	0.009	2.102	1.937	0.117/–0.001	0.051/–0.002	7.722	0.966/2.001	0.296/6.005
	Co(5)	–0.024	2.192	1.996	0.159/–0.001	0.040/–0.002	7.744	1.002/2.001	0.273/6.005
	Co(6)	–0.007	1.393	1.234	0.116/–0.001	0.046/–0.002	7.834	0.762/2.001	0.403/6.007

is presented as a solid vertical line and shifted to zero. As evident from the figure, the d-orbit curves of these clusters are narrow and sharp, which indicates that distribution of d electrons is relatively localized. The electronic states between –4 and 2 eV mainly come from d electron state, whereas the contributions from s and p electron states are very little. If the curves of spin-up density and spin-down density show low symmetry, it implies that there exist many unpaired electrons, leading to a large contribution to magnetic moment. As shown in figure 7, the curves of Cu_6NO and Cu_5CoNO clusters show high symmetry; hence, the magnetism is pretty small. The symmetry becomes lower with increasing concentration of Co atoms; hence, the magnetic moment increases. In general, the relative shift between the spin-up and spin-down bands can indicate the degree of spin exchange splitting. The larger the degree of spin exchange split, the lager the magnetism of cluster. As shown in the figure, all d electron bands have significant shift. The order of the shift degree is Cu_6NO, $Cu_5CoNO < Cu_4Co_2NO < Cu_3Co_3NO < Co_6NO < Cu_2Co_4NO < CuCo_5NO$, indicating that with the increase of Co atoms doping in the clusters, the shift gets larger, which agrees well with the earlier total magnetic moment analysis.

The electron spin density around each atom for these clusters is also discussed in figure 8, where the blue and yellow represent spin-up and spin-down electronic states, respectively. The larger the electron spin density, the more the unpaired electrons around atoms, indicating that the local magnetic moment is larger [22,23]. As shown in figure 8, electron spin density of N, O and Cu atoms is quite small to be observed, which implies that the number of unpaired electrons is quite small. In conclusion, N, O and Cu atoms make quite a small contribution to the magnetic moment, whereas Co atoms provide the majority contribution to magnetism, which is consistent with the Mulliken populations analysis. Cu_6NO, Cu_5CoNO, Cu_4Co_2NO, Cu_3Co_3NO, Cu_2Co_4NO and $CuCo_5NO$ clusters have only spin-up electronic states; moreover, the spin-up density gets larger, suggesting that these clusters have more and more unpaired electrons. Hence, the

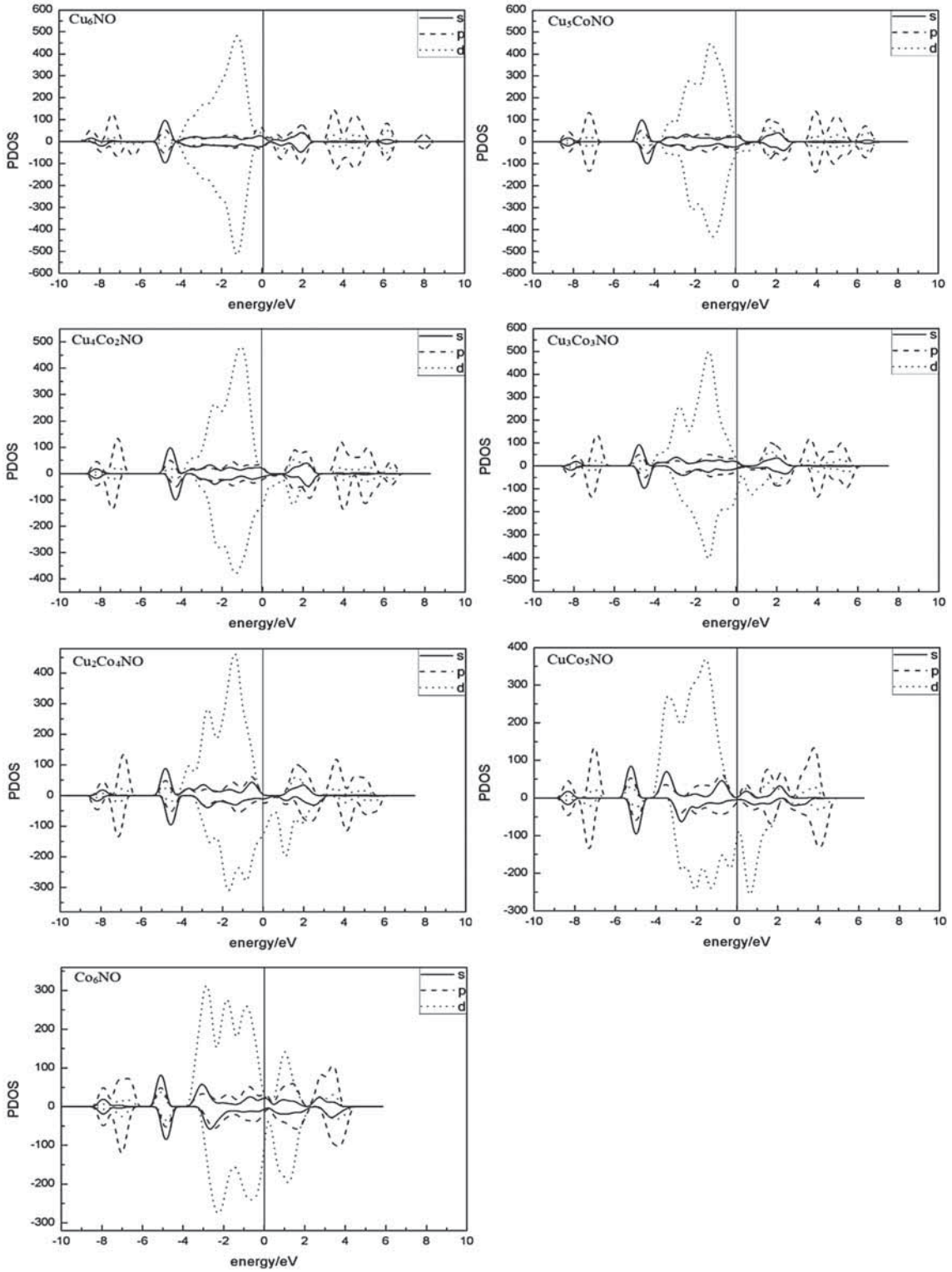

Figure 7. The PDOS of Cu_mCo_nNO ($m + n = 6$) clusters at ground state.

magnetism gets higher as a function of Co concentration, which corresponds well with the analysis of magnetic moment in figure 7. Co_6NO clusters have both up-spin and down-spin electronic states. However, the down-spin region is distributed at only two Co atoms and up-spin region has a wide distribution area, indicating that much more up-spin unpaired

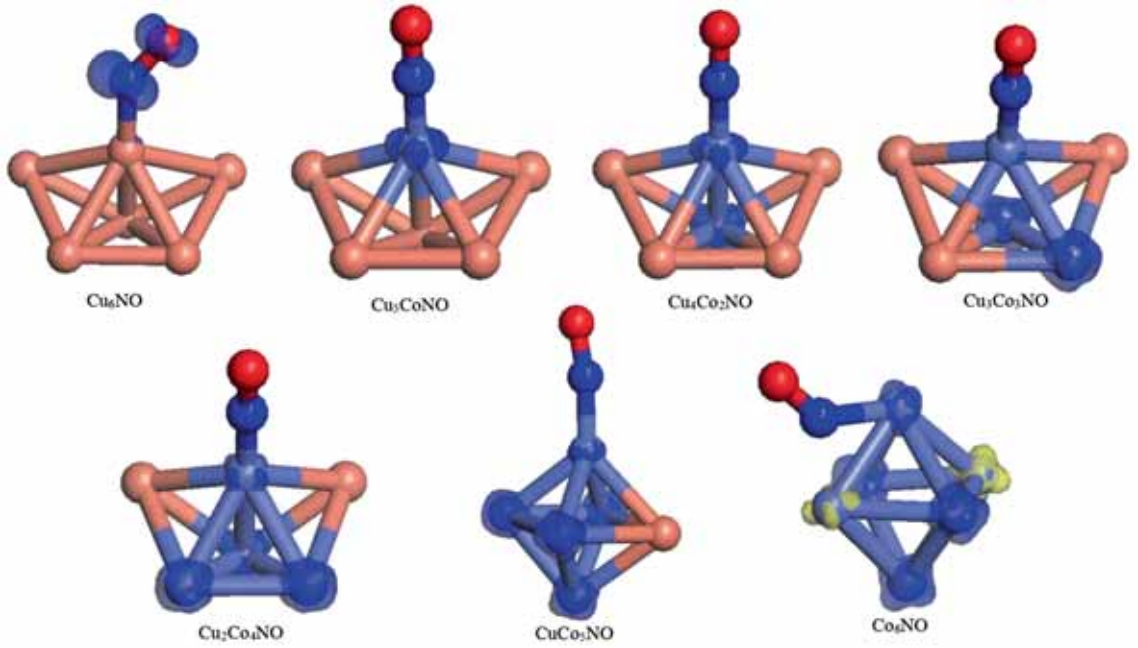

Figure 8. The electron spin density maps of Cu_mCo_nNO ($m + n = 6$) clusters at ground state.

electrons exist than down-spin unpaired electrons; thus, total magnetic moment of Co_6NO clusters has a large positive value.

4. Conclusion

A theoretical study of NO adsorption on Cu_mCo_n ($2 \leq m + n \leq 7$) clusters was carried out using a density functional method. Generally, NO is absorbed at top sites via the N atom, while NO of Cu_3NO and Cu_5NO clusters is located at the bridge site via the N atom. The adsorption energy of Co_2NO, Co_3NO, Cu_2Co_2NO, Co_5NO, Cu_2Co_4NO and Cu_6CoNO clusters is relatively larger than that of their neighbouring clusters, indicating that the interaction of NO and these alloy clusters is stronger. NO of Cu_mNO ($m =$ 1–7) and Co_6NO clusters are all negatively charged; hence, the charge of these clusters is transferred from alloy clusters to NO molecules. The vibration frequency of N–O bond is lower than that of a single NO molecule, which implies that the N–O bond is weakened and the activity is enhanced after adsorption. The $\Delta_2 E$ values of Cu_2CoNO, Cu_3CoNO, Cu_2Co_2NO, Cu_3Co_3NO and $CuCo_5NO$ clusters are relatively larger than others, indicating that these five clusters are much more stable. CuCoNO, Co_3NO, Cu_3CoNO, Cu_2Co_3NO, Cu_3Co_3NO and Cu_6CoNO clusters display higher energy gaps, which means that the chemical stability of these clusters is stronger compared with neighbouring clusters. Magnetic and electronic properties are also discussed. In general, the magnetic moments increase as the number of Co atoms doped in pure Cu clusters increases. This arises from charge transfer and spd hybridization, resulting in the original electron pairing changes. N, O and Cu atoms make quite small contribution to the magnetism.

Acknowledgements

This project was supported by the National Natural Science Foundation of China (Grant Number 21207051) and the Graduate Student Research Innovation Program of Jiangsu University of Science and Technology (Grant Number YCX15S-26) and Postgraduate Research & Practice Innovation Program of Jiangsu Province (Grant No. KYCX17_1838).

References

[1] Martínez A, Jamorski C, Medina G and Salahub D R 1998 *J. Phys. Chem. A* **102** 4643
[2] Grönbeck H, Hellman A and Gavrin A 2007 *J. Phys. Chem. A* **111** 6062
[3] Yan Z, Zuo Z, Li Z and Zhang J 2014 *Appl. Surf. Sci.* **321** 339
[4] Lacaze-Dufaurea C, Roquesb J and Mijoulea C 2011 *J. Mol. Catal. A: Chem.* **341** 28
[5] Fan C and Xiao W D 2013 *Comput. Theor. Chem.* **1004** 22
[6] Ding X, Li Z and Yang J 2004 *J. Phys. Chem. A* **121** 2558
[7] Endou A, Ohashi N and Takami S 2000 *Top. Catal.* **11–12** 271
[8] Matulis V E, Palagin D M, Mazheika A S and Ivashkevich O A 2011 *Comput. Theor. Chem.* **963** 422
[9] Nahali M and Gobal F 2011 *Mol. Phys.* **109** 229
[10] Valadbeigi Y, Farrokhpour H and Tabrizchi M 2015 *J. Chem. Sci.* **127** 2029

[11] Janssens E, Hoof T V and Veldeman N 2006 *Int. J. Mass Spectrom.* **252** 38
[12] Heard C J and Johnston R L 2013 *Eur. Phys. J. D* **67** 1
[13] Li G, Wang Q and Li D 2008 *Phys. Lett. A* **372** 6764
[14] Sebetci A 2012 *Comput. Mater. Sci.* **58** 77
[15] Yuan D W, Liu C and Liu Z R 2014 *Phys. Lett. A* **378** 408
[16] Guo W, Tian W Q and Lian X 2014 *Comput. Theor. Chem.* **1032** 73
[17] Qin J P, Liang R R and Lv J 2014 *Acta Phys. Sin.* **63** 133102
[18] Lu Q L, Zhu L Z and Ma L 2005 *Chem. Phys. Lett.* **407** 176
[19] Lv J, Bai X and Jia J F 2012 *Physica B: Condens. Matter* **407** 14
[20] Matulis V E and Ivaskevich O A 2006 *Comput. Mater. Sci.* **35** 268
[21] Grybos R and Benco L 2009 *J. Chem. Phys.* **130** 51
[22] Zheng X Y, Zhang X R and Zhang L L 2015 *Int. J. Mod. Phys. B* **29** 1550184
[23] Zhang X R, Luo M and Zhang F X 2015 *Bull. Mater. Sci.* **38** 425